Applied Physics Letters

Photo-charging polymeric sodium-ion cell based on YSZ/PVDF film

Cite as: Appl. Phys. Lett. **115**, 183904 (2019); https://doi.org/10.1063/1.5123784
Submitted: 09 August 2019 . Accepted: 21 October 2019 . Published Online: 31 October 2019

Farha Khatun, Pradip Thakur, Biswajoy Bagchi, and Sukhen Das

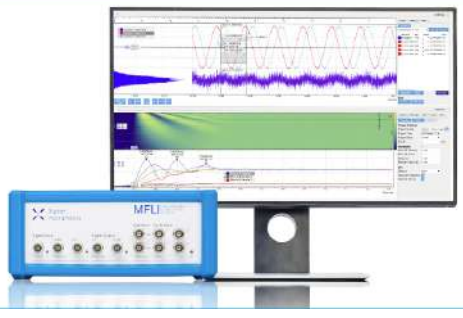

AIP Publishing

Applied Physics Letters ARTICLE scitation.org/journal/apl

Photo-charging polymeric sodium-ion cell based on YSZ/PVDF film

Cite as: Appl. Phys. Lett. **115**, 183904 (2019); doi: 10.1063/1.5123784
Submitted: 9 August 2019 · Accepted: 21 October 2019 ·
Published Online: 31 October 2019

Farha Khatun,[1] Pradip Thakur,[2,a)] Biswajoy Bagchi,[3] and Sukhen Das[1]

AFFILIATIONS

[1]Department of Physics, Jadavpur University, Kolkata 700032, India
[2]Department of Physics, Netaji Nagar College for Women, Kolkata 700092, India
[3]Department of Medical Physics and Biomedical Engineering, University College London, London, WC1E 6BT, United Kingdom

[a)]**Author to whom correspondence should be addressed:** pradipthakurju@gmail.com. **Tel.:** +919830366215

ABSTRACT

A cost-effective, light-weighted, and easy to handle photochargeable Na-ion power cell (NPPC) has been demonstrated by integrating solar active solid electrolyte poly(vinyl alcohol)-carbon black-V_2O_5-Na_2SO_4 and a high dielectric YSZ/PVDF film in a very simple and unique way. An open circuit voltage of ∼1.18 V is obtained under photocharging of the NPPC by light with an intensity of ∼110 mW/cm^2. The discharging phenomenon is investigated at a constant discharge current density of ∼0.63 mA/cm^2. The reversible charging-discharging nature of the device is recorded repeatedly for 200 cycles to investigate the storage capacity. A maximum capacitance of ∼2.84 mF/cm^2 is obtained with an energy density and a power density of ∼5.6 mWhr/m^2 and ∼ 7.4 W/m^2, respectively. The high storage impact of NPPC is realized in practical by glowing blue light emitting diodes for two days with high intensity.

The utilization of clean and renewable energy sources such as sunlight, wind, water, biomass energies, and geothermal energy is significantly increased due to the overall energy crisis.[1] So researchers are highly focused on the production of efficient, low-cost energy storage technologies for large-scale clean energy implementation. At present, different types of batteries (lithium and sodium ion batteries) have attracted tremendous attention in the application of medium/wide-scale energy storage arena.[2] But scientists are very much interested to develop some innovative idea of both renewable energy conversion and storage in one system.

Improvement of photovoltaic solar cells by using dye is a very good option for the restoration of the natural fossil fuels (petroleum, coal, etc.). Although the progress of lithium-ion/sodium-ion based energy storage devices, sodium ion capacitors, etc.,[3] is burgeoning, the photovoltaic self-charging polymeric composite system based on the sodium ion, which is capable of undergoing both solar to electrical energy conversion with storage, is rarely reported until now. Some kinds of dye sensitized solar cells, self-charging photocapacitors, etc., were already reported by Ma *et al.*, Guo *et al.*, and Miyasaka *et al.*[4,5] Previously, we have evaluated some different types of photoinduced power cells with the help of high dielectric polymer composite films and nanoparticle dye in combination with light absorbing organic dye with superior storage capability.[6–8]

As an electroactive polymer, poly(vinylidene fluoride)(PVDF) ([-CH2-CF2-]n) and its copolymers are very well known for their flexibility and cost effectiveness for the application of piezoelectric nanogenerators, capacitors, thin film transistors, grid leveling, rail runs, nonvolatile memories, sensors, and actuators, in biomedical fields, and also photopower banks. PVDF is an electroactive semicrystalline polymer with five polymorphs α, β, γ, δ, and ε and shows piezoelectric, pyroelectric, and ferroelectric properties with very good thermal stability and chemical resistance.[9–11] Among the five crystalline phases, the β phase is the most electroactive phase since it contains the *all trans* (TTTT) planar zigzag arrangement with the orthorhombic unit cell matrix.[12]

So for the advancement of the β phase with good dielectric properties, we choose a ceramic compound yttria stabilized zirconia (YSZ), which is a cubic crystal of zirconium oxide stabilized by the addition of yttrium oxide as a filler of PVDF.[13] YSZ is a ceramic material, which has many applications in the case of jet engines, gas turbines, etc., due to its hardness and chemical structure, and it is also applicable as an electroceramic in different types of fuel cells for its ion-conducting properties. Here, a Na-ion based photovoltaic self-charging energy storage system, i.e., a photopower cell, is developed by using the initially prepared dielectric improved YSZ-PVDF composite film and a mixture of poly(vinyl alcohol) (PVA), vanadium pentoxide (V_2O_5),

and carbon black in the presence of sodium sulfate (Na_2SO_4) as an electrolyte. At present, the sodium base electrochemical device has achieved a very good response for its harmless nature, longevity, simple and cost-effective preparation method and is also comparable with the Li- ion energy system due to the dense energy-capacity.[3] The fabricated energy system based on the Na ion is named as a photoinduced Na-ion power cell (NPPC).

Typically, 20 mass% YSZ is mixed with the solution of 200 mg of PVDF and 5 ml of dimethyl sulfoxide (DMSO) under vigorous magnetic stirring for 12 h followed by 30 min of ultrasonication. The YSZ incorporated PVDF (PYZ20) films of thickness ~20 μm are prepared after 6 h of drying of the mixed solution in a dust-free hot air oven at 100 °C. A similar process is also followed to prepare the pure PVDF films. We have used the PYZ20 composite films as an insulating separator to fabricate the NPPC. The photoabsorbing material, i.e., the solar part of NPPC, is prepared by combining 40 mg/ml PVA, 40 mg/ml carbon black, 2 mg/ml V_2O_5, and 100 mg/ml Na_2SO_4 in water and stirred for 12 h at 60 °C. After preparation of the electrolyte, the sticky solution is placed on the FTO coated glass and the PYZ20 high dielectric film is attached on it with aluminum (0.2 cm × 0.2 cm). The typical area of the device is (0.2 cm × 0.2 cm), i.e., 0.04 cm^2. Then, two wires are connected with FTO glass and Al, which are used as acting and counter electrodes, respectively.

Initially, the nucleation of the electroactive β phase is ensured by X-ray diffraction (XRD) patterns [Fig. 1(a)] of YSZ loaded PVDF samples using an X-ray diffractometer (Model-D8, BrukerAXS, Inc, Madison, WI). The pure PVDF film confirms about the existence of the nonpolar α phase due to the presence of the diffraction peaks around 17.6° (100), 18.3° (020), 19.9° (021), and 26.6° [(201), (310)], while the formation of crystalline β polymorphs of PYZ20 is ensured due to the clear peak at 20.8° [(110), (200)].[14] The intensity ratio of peaks $I_{20.5}$ and $I_{18.2}$ is evaluated (~ 0.96 for PVDF ~ 4.36 for PYZ20), which shows the amount of α and β phases in the pure and PYZ20 composite thin films. The Fourier transform infrared (FTIR-8400S, Shimadzu) spectra [Fig. 1(b)] of pure PVDF and YSZ incorporated

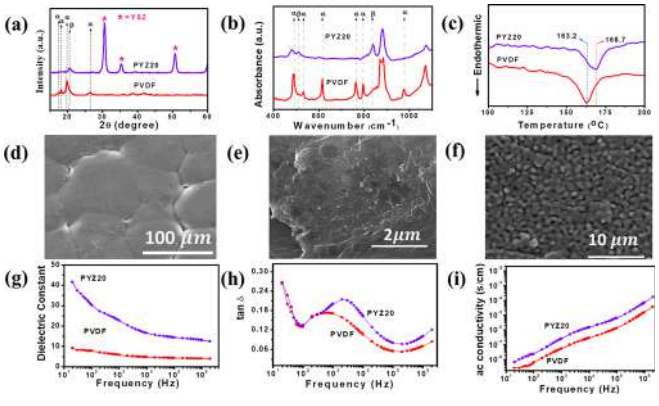

FIG. 1. (a) X-Ray diffraction patterns of pure PVDF and YSZ incorporated PVDF composite thin films, (b) FTIR spectroscopy of pure PVDF and PYZ20 thin films, (c) DSC thermographs of pure PVDF and YSZ modified PVDF thin films, (d) and (e) FESEM microstructures of pure PVDF and YSZ modified PVDF films, and (f) FESEM image of the YSZ particles. Variation of the (g) dielectric constant, (h) tangent loss, and (i) ac conductivities with the frequency of pure PVDF and PYZ20 composite films.

PVDF films show the absorbance bands at 489 cm^{-1} (CF_2 wagging), 533 cm^{-1} (CF_2 bending), 615 and 764 cm^{-1} (CF_2 bending and skeletal bending), and 795 and 975 cm^{-1} (CH_2 rocking) for the α-phase in the pure sample and 475 cm^{-1} (CF_2 deformation), 510 cm^{-1} (CF_2 stretching), 600 cm^{-1} (CF_2 wag), and 840 cm^{-1} (CH_2 rocking, CF_2 stretching and skeletal C–C stretching) for the formation of the β phase in the PYZ sample.[14] The percentage of the crystalline β phase is estimated (~76%) for the PYZ20 thin films by using the Lambert–Beer law [Eq. (S1)].

The origination of the crystalline β phase and also the phase transition activity are justified by the thermal technique and differential scanning calorimetry (DSC-60, Shimadzu (Asia Pacific) Pte. Ltd., Singapore). A shift of ~5.5 °C in melting temperature is seen due to some change in the molecular orientation and crystalline structure of the PYZ films with respect to that of the pure PVDF film (~163.2 °C) from the DSC thermographs [Fig. 1(c)]. This is a clear verification of the electroactive β phase nucleation, which is already confirmed by the XRD and FTIR techniques.[14,15]

The microstructures of the unblended PVDF and YSZ incorporated PVDF samples are obtained using a field emission electron microscope (FESEM) (INSPECT F50, Netherlands). A spherical structure has a diameter of ~ 50–70 μm for pure PVDF. Uniform distribution of the YSZ particles throughout the samples has been observed in the FESEM image of PYZ20 shown in Fig. 1(e). Figure 1(f) shows the pure YSZ nanoparticles with a diameter of ~30–50 nm.[16]

The dielectric behavior (dielectric constant, tangent loss, and ac conductivity) of the neat PVDF and YSZ modified PVDF composite samples is investigated within the frequency range of 20Hz–2 MHz by using a digital LCR meter (Agilent, E4980A). At first, the capacitance is measured, and then we have used Eqs. (S2) and (S3) to calculate the dielectric constant and ac conductivity, respectively. The maximum value of the dielectric constant is found to be ~ 42 for the PYZ20 composite films, while the value is ~ 9 for the pure PVDF films in the lower frequency region of 20 Hz [Fig. 1(g)]. A constancy of the dielectric value is seen for the pure PVDF, and a gradual decrement is noticed for the PYZ20 sample with increasing frequency. The high value of the dielectric constant can be interpreted by the MWS interfacial polarization, i.e., the large number of dipoles formed due to the charge carrier augmentation.[15,17,18] The tangent loss (tan δ) values of the neat PVDF and PYZ composite samples are shown in Fig. 1(h). According to the figure, the tan δ value initially decreases and then a sharp increasing behavior is obtained with the increment of the frequency. This sharp increment may be comparable with the dielectric relaxation peak, and the fluctuating behavior arises due to the Debye-like relaxation phenomenon in the samples due to the externally applied field.[19] The variation of the ac conductivity is nearly unchanged in the low frequency region and increased linearly in the higher frequency range [Fig. 1(i)] for the pure and composite samples.[15]

On the basis of the aforementioned characterization, it is confirmed that the high dielectric (~ 42) and electroactive (~76%) PYZ20 composite films have been synthesized. Due to its large dielectric value, the PYZ20 composite thin film is the most proper choice for the development of NPPC as an insulating material. The NPPC is designed by using a FTO coated glass that contains the photoelectron generator composite electrolyte mixture of PVA/carbon black/V_2O_5/Na_2SO_4 adjoined with the high dielectric storage material YSZ improved PVDF film (PYZ20) of average thickness ~20 μm and dimensions

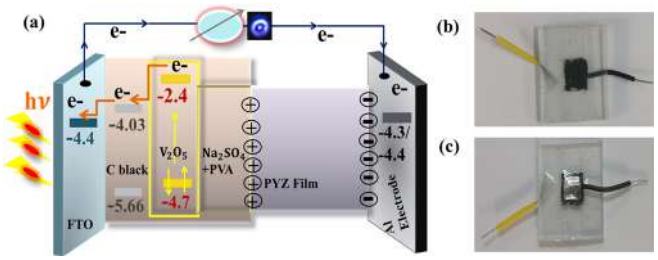

FIG. 2. (a) Schematic diagram of photocharge carrier generation and storage mechanism of the NPPC with HOMO and LUMO energy states; (b) Digital image of upper and lower sides of the NPPC.

0.20 cm × 0.20 cm. Sodium salt (Na_2SO_4) and PVA are used in the solar part to form the gel type electrolyte medium for supplying the charge carriers.[20] After the fabrication, the storage system is charged by a 40 W tungsten bulb of intensity 110 $mWcm^{-2}$ with covering ultraviolet and infrared light eliminating filters.

The working mechanism of the NPPC is presented symbolically in Fig. 2(a) with the help of the HOMO/LUMO structure of the solar material. The digital photographs of both the sides of NPPC are also displayed in Figs. 2(b) and 2(c). Two processes are simultaneously occurring in the same device, one is the photoelectron generation by the light absorbing part and the other is the deposit of the photoelectrons across the high dielectric PYZ20 thin film. The photovoltaic behavior of the NPPC is studied on the basis of photocharge carrier produced by the solar portion PVA/carbon black/V_2O_5/Na_2SO_4 on the conducting electrode FTO coated glass and the device storage capacity for the insulating PYZ20 sample attached with the counter electrode Al.

The self-charging and discharging behavior of the NPPC is represented by a graphical plot of the voltage against time in Fig. 3(a). After illuminating the device under the tungsten bulb filament, the electrons in the HOMO energy state (∼ −4.7 eV) of V_2O_5 will be excited to the LUMO energy state (∼−2.4 eV) due to absorption of the photon particles ($h\nu$).[21,22] After this excitement of the charge carriers to the higher energy level, it will be instantly transferred to the FTO glass through the carbon black since its LUMO level (∼−4.03 eV) is consequently lower than that of V_2O_5.[23,24] The carbon black is mixed with the solar material to make a continuous and easy conduction of the photocharge carriers to the electrode. Since both the electrodes are connected through a copper wire, the charge carriers will flow to the Al counter electrode and will be deposited at the adjoining surface of the PYZ20 thin film and Al and cannot be conducted further due to the high dielectric insulating PYZ20 composite sample. So there will be a surplus of negative charges at the Al electrode, and with respect to this, FTO will act as a positive electrode. During the process, a deficiency of photo charge carriers must be created by V_2O_5, which is fulfilled by the Na based viscous electrolyte gel in addition to PVA. Although different types of Na compounds (Na_2Sn_4, etc.) are used as a battery anode or cathode material and ($NaPF_6$, $NaCO_3$, $NaCLO_4$ etc.) as electrolytes for the Na ion batteries, here Na_2SO_4 is chosen as an electrolyte composite to develop a unique storage system (NPPC) based on sodium.[3]

V_2O_5 is a very well known hole transporter and largely used in solar cells. We are just trying to explain our device mechanism using the HOMO-LUMO state under solar light exposure. In aqueous medium, V^{5+} can be reduced to the V^{4+} state due to high oxidizing power of V^{5+} in V_2O_5. Here is some possibility of PVA in PVA/Na_2SO_4 acting as an electron donor along with Na_2SO_4 as PVA is a well-known electron donor and capping reagent.[7] We here just describe all possible electron replenishing mediators of V_2O_5. In aqueous medium, V^{5+} can be reduced to the V^{4+} state due to high oxidizing power of V^{5+} in V_2O_5.[2,22,25–28] A simultaneous reduction-oxidation process will take place in the solar part under visible light, and the photogenerated holes will be reloaded by the electron supplied from ionic intermediate electrolyte solution PVA/Na_2SO_4. The proposed mechanism may be as follows:

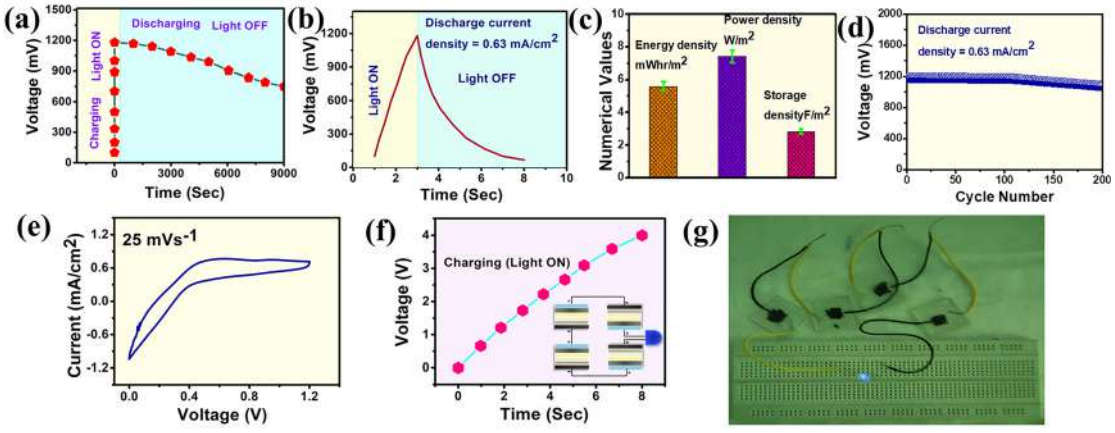

FIG. 3. (a) and (b) Self-charging and discharging behavior (V-t curves) of the NPPC fabricated by the PYZ20 high dielectric composite thin film as a function of time under light illumination and dark conditions, (c) the comparative values of energy density, power density, and storage density of NPPC, (d) investigation of the recyclability, i.e., long lastingness (200 cycles) of NPPC by self-charging and discharging behavior, (e) the curve of cyclic voltammetry with 0–1.2 V at a voltage change of 25 mV/s, (f) self-charging (V-t) curve of four serially connected NPPC under light illumination with the schematic diagram, and (g) the digital photograph of the glowing of the a blue LED by serially connected four NPPCs as a power cell.

$$\mathbf{PVA} \leftrightarrow \mathbf{PVA}^{-}$$

$$V_2O_5(\text{in aqueous}) + Na_2SO_4 + \mathbf{h\nu} \rightarrow [V_2O_{5-x}]\left[SO_4^{2-}\right] + \mathbf{Na}^{+} + \mathbf{xe}^{-},$$

$$V_2O_5(\text{in aqueous}) + \text{PVA} + \mathbf{h\nu} \rightarrow [V_2O_{5-x}][\text{PVA}^{-}] + \mathbf{xe}^{-}.$$

After the completion of the charging process, the maximum open circuit voltage of 1.18 V is obtained within 3 s because of the potential difference between the two electrodes. The fast charging phenomenon is basically due to the continuous and vigorous outflow of the photo-charge carriers provided through Na based electrolyte. The figure shows a slow discharging process in dark ambience, which is the implication of the good storage capability (~ 2.84 mF/cm^2) [Eq. (S5)] of the NPPC due to the superior electrochemical features of sodium regarding charging-discharging activity. After that, the device is discharged in 5 s through a constant discharge current density ($\sim$0.63 mA/cm^2) [Fig. 3(b)] with a charge density of 3.15 mC/cm^2 [Eq. (S4)]. According to Fig. 3(c), the maximum output energy attained for NPPC is ~ 5.6 mWhr/m^2 with a power density of 7.4 W/m^2 [Eqs. (S6) and (S7)]. The necessary equations and comparison with previously reported different types of photopower cells (Table S1) are supplied in the supplementary material. The long lastingness or durable nature of the Na based storage device is investigated by observing the charging–discharging recyclable performance for 200 cycles [Fig. 3(d)], and it is noticeable that only an 8.6% drop of photovoltage has observed for the NPPC after 200 cycles (20 days). The cyclic voltammetric (CV) behavior of the NPPC has been checked and is represented in Fig. 3(e), and the graphical behavior confirms about the good electrochemical stability of the Na based photo power cell (NPPC). A potential range of 0–1.2 V at a scan rate of 25 mV/s has been used for the CV measurement. The realistic application of NPPC is also explored by illuminating a blue light emitting diode (LED) through a connection of four NPPCs in series [Fig. 3(g)]. High energy density with good storage capacity of Na/PVA dependent NPPC is justified by the intense and steady glow of the LED for two days.

So initially, high dielectric and electroactive YSZ incorporated PVDF films are prepared with 76% β phase and 42 dielectric constant via a simple solution casting method. Then Na_2SO_4/PVA combined electrolyte based on a unique, low-cost, and light-weighted photo induced Na-ion power cell (NPPC) has been fabricated by using the high dielectric PYZ20 thin film as a storage material. We have achieved a maximum voltage of 1.18 V within 3 s with an excellent power density of 7.4 W/m^2.

See the supplementary material for synthesis of YSZ, its characterization (XRD and SEM), the required materials, necessary equations, and comparison table. Demonstration of glowing commercially available blue LEDs using NPPC is supplied as Video S1.

The authors are thankful to the Department of Higher Education, Science & Technology and Biotechnology, Government of West Bengal, India, and University Grants Commission (UGC), India, for providing financial assistances.

REFERENCES

[1]L. Gao, S. Chen, L. Zhang, and X. Yang, J. Alloys Compd. **766**, 284–290 (2018).
[2]E. Lim, C. Jo, M. S. Kim, M.-H. Kim, J. Chun, H. Kim, J. Park, K. C. Roh, K. Kang, S. Yoon, and J. Lee, Adv. Funct. Mater. **26**, 3711 (2016).
[3]M. D. Slater, D. Kim, E. Lee, and C. S. Jhonson, Adv. Funct. Mater. **23**, 947 (2013).
[4]T. Miyasakaa and T. N. Murakami, Appl. Phys. Lett. **85**, 3932 (2004).
[5]W. Guo, X. Xue, S. Wang, C. Lin, and Z. L. Wang, Nano Lett. **12**, 2520 (2012).
[6]F. Khatun, N. A. Hoque, P. Thakur, N. Sepay, S. Roy, B. Bagchi, A. Kool, and S. Das, Energy Technol. **5**, 2205 (2017).
[7]S. Roy, P. Thakur, N. A. Hoque, B. Bagchi, N. Sepay, F. Khatun, A. Kool, and S. Das, Appl. Mater. Interfaces **9**, 24198 (2017).
[8]F. Khatun, P. Thakur, A. Kool, S. Roy, N. A. Hoque, P. Biswas, B. Bagchi, and S. Das, Langmuir **35**, 6346 (2019).
[9]X. Xue, P. Deng, S. Yuan, Y. Nie, B. He, L. Xing, and Y. Zhang, Energy Environ. Sci. **6**, 2615 (2013).
[10]Y. S. Kim, Y. Xie, X. Wen, S. Wang, S. J. Kim, H. K. Song, and Z. L. Wang, Nano Energy **14**, 77 (2015).
[11]P. Thakur, A. Kool, N. A. Hoque, B. Bagchi, F. Khatun, P. Biswas, D. Brahma, S. Roy, S. Banerjee, and S. Das, Nano Energy **44**, 456 (2018).
[12]P. Thakur, A. Kool, B. Bagchi, S. Das, and P. Nandy, Appl. ClaySci. **99**, 149 (2014).
[13]B. Bagchi and R. N. Basu, J. Alloys Compd. **647**, 620 (2015).
[14]P. Martins, A. C. Lopes, and S. Lanceros-Mendez, Prog. Polym. Sci. **39**, 683 (2014).
[15]S. Lanceros-Méndez, J. F. Mano, A. M. Costa, and V. H. Schmidt, J. Macromol. Sci., Part B **40**, 517 (2001).
[16]P. Thakur, A. Kool, B. Bagchi, N. A. Hoque, S. Das, and P. Nandy, RSC Adv. **5**, 28487 (2015).
[17]A. Scho.nhals, H. Goering, F. R. Costa, U. Wagenknecht, and G. Heinrich, Macromolecules **42**, 4165 (2009).
[18]F. Carpi, G. Gallone, F. Galantini, and D. D. Rossi, Adv. Funct. Mater. **18**, 235 (2008).
[19]P. Lunkenheimer, V. Bobnar, A. V. Pronin, A. I. Ritus, A. A. Volkov, and A. Loid, Phys. Rev. B **66**, 052105 (2002).
[20]K. Lu, D. Li, X. Gao, H. Dai, N. Wang, and H. Ma, J. Mater. Chem. A **3**, 16013 (2015).
[21]P. Biswas, N. A. Hoque, P. Thakur, Md. M. Saikh, S. Roy, F. Khatun, B. Bagchi, and S. Das, ACS Sustainable Chem. Eng. **7**, 4801 (2019).
[22]S. Rafique, S. M. Abdullah, W. E. Mahmoud, A. A. Al-Ghamdi, and K. Sulaiman, RSC Adv. **6**, 50043 (2016).
[23]I. M. L. Billas, C. Massobrio, M. Boero, M. Parrinello, W. Branz, F. Tast, N. Malinowski, M. Heinebrodt, and T. P. Martin, J. Chem. Phys. **111**, 6787 (1999).
[24]K. Komeyama, T. Yamada, R. Igawaa, and K. Takaki, Chem. Commun. **48**, 6372 (2012).
[25]L. Zhang, C. Jiang, C. Wu, H. Ju, G. Jiang, W. Liu, C. Zhu, and T. Chen, ACS Appl. Mater. Interfaces. **10**, 27098 (2018).
[26]J. Livage, Mater. Res. Bull. **26**, 1173 (1991).
[27]J. Livage, Chem. Mater. **3**, 578 (1991).
[28]I. Hancox, L. A. Rochford, D. Clare, M. Walker, J. J. Mudd, P. Sullivan, S. Schumann, C. F. McConville, and T. S. Jones, J. Phys. Chem. C **117**, 49 (2013).